

In vitro and *In silico* studies on inhibitory effects of curcumin on multi drug resistance associated protein (MRP1) in retinoblastoma cells

Seethalakshmi Sreenivasan¹ & Sathyabaarathi Ravichandran², Umashankar Vetrivel^{2*}, Subramanian Krishnakumar¹

¹L&T Department of Ocular Pathology, Vision Research Foundation, Sankara Nethralaya, 18, College Road, Nungambakkam, Chennai - 600 006, India; ²Centre for Bioinformatics, Vision Research Foundation, Sankara Nethralaya, 18, College Road, Nungambakkam, Chennai - 600 006, India; Umashankar Vetrivel -Email: vumashankar@gmail.com; *Corresponding authors

Received December 17, 2011; Accepted December 20, 2011; Published January 06, 2012

Abstract:

Multi Drug Resistance (MDR) is one of the major causes of chemotherapy failure in human malignancies. Curcumin, the active constituent of *Curcuma longa* is a proven anticancer agent potentially modulating the expression and function of these MDR proteins. In this study, we attempted to test curcumin for its potential to inhibit the expression and function of multidrug resistance associated protein 1 (MRP1) in retinoblastoma (RB) cell lines through western blot, RT-PCR and functional assays. *In silico* analysis were also performed to understand the molecular interactions conferred by curcumin on MRP1 in RB cells. Western blot and RT-PCR analysis did not show any correlation of MRP1 expression with increase in concentration of curcumin. However, inhibitory effect of curcumin on MRP1 function was observed as a decrease in the efflux of fluorescent substrate. Moreover, Curcumin did not affect 8-azido-ATP-biotin binding to MRP1 and it also showed inhibition of ATP-hydrolysis stimulated by quercetin, which is indicative of curcumin's interaction with the substrate binding site of MRP1. Furthermore, homology modelling and docking simulation studies of MRP1 also provided deeper insights into the molecular interactions, thereby inferring the potential binding mode of curcumin into the substrate binding site of MRP1.

Keywords: Curcumin, ATP-Binding Cassette, Retinoblastoma, Multi-Drug Resistance Protein, Molecular Docking, Binding analysis

Background:

Retinoblastoma (RB) is the most common primary intraocular malignancy of children [1]. Chemotherapy is the treatment of choice following enucleation in patients with optic nerve and choroids invasion and also orbital extension [2]. One of the major problems related with chemotherapy drugs in RB is resistance against anticancer agents [3]. Over-expression of P-glycoprotein (P-gp), Multidrug Resistance-associated Protein 1 (MRP1), and Lung Resistance-related Protein (LRP) are associated with development of multi drug resistance (MDR) in various cancer cells [4]. MRP belongs to the ATP-binding cassette (ABC) transporter family [1]. The MRP family consists of nine members (MRP1-9), all these proteins contain hydrophobic membrane spanning domains (TMDs) and ISSN 0973-2063 (online) 0973-8894 (print) Bioinformation 8(1): 013-019 (2012)

cytoplasmic nucleotide-binding domains (NBDs), wherein, NBD is responsible for ATP binding/hydrolysis [5]. Earlier studies have reported that MRP1 expression is associated with the rare failure of chemotherapy in RB tumor despite the use of cyclosporine [6]. It was also reported that cells which highly express MRP1 show resistance to anti-cancer drugs like vinca alkaloids, anthracyclines and epipodophyllotoxins [7]. Chemotherapeutic treatments have been associated with adverse side effects and dose limiting toxicity [8]. Many natural compounds have been reported to interact with the transmembrane transporters and also found to sensitize cancer cells to anti-cancer drugs [9]. In the recent decades, extensive research has been done on curcumin to establish its biological and pharmacological activities. It has been reported that

curcumin confers therapeutic and chemo-sensitization effect, and also reported to have modulating role on MDR proteins [10]. These findings suggest the curcumin's interaction with the conserved functional domains of the drug resistance proteins, thereby inhibiting their function. However, the molecular mechanism behind the physiological effects of curcumin is not well-studied. Hence, in this present study, we have selected Y79 RB cells as an *in vitro* model for RB cancer and studied the effect of curcumin on MRP1 expression and function. Further *in silico* approaches have also been studied to deduce the inhibitory binding mode of curcumin on MRP1 protein.

Methodology:

Reagents

Curcumin (Sigma) were dissolved in dimethyl sulphoxide (DMSO) and stored at -20°C. Cell culture materials were purchased from Invitrogen (Carlsbad, CA, USA). All other chemicals and reagents were of the highest grade commercially available.

Cell culture:

The Y79 cell line was obtained from the American Type Culture Collection (Manassas, VA, USA) and maintained in a RPMI-1640 medium supplemented with 20% fetal bovine serum with 50ng/mL of streptomycin and 1.25ng/mL of Amphotericin B at 37°C in a humidified atmosphere with 95% O₂ and 5% CO₂.

Effects of curcumin on MRP1 expression in RB cell line

RT-PCR studies for MRP1 on curcumin treated (2-10µM) & untreated Y79 RB cells were performed with 2µg of total RNA from each sample. The cDNA products were amplified for 35 cycles using specific primers and the amplification product was fractionated by electrophoresis using 2% agarose gel containing 0.5% Ethidium Bromide (Table 1, see supplementary material). Further, for protein expression studies, the curcumin treated and untreated cell lysates (50µg) were loaded onto 8% polyacrylamide gels and the western blot for MRP1 (1:2000) and β-actin (1:4000) was performed. Protein bands were visualized using a chemiluminescence kit. The relative amount of MRP1 mRNA and protein expression was determined by densitometer.

MRP1 functional study using calcein-AM by flow cytometry

The accumulation of calcein-AM, which is a fluorescent substrate for MRP1, was used for the functional study. 5x10⁴ Y79 cells were collected and 0.5µM of calcein-AM was added in the presence and absence of 10µM curcumin and incubated at 37°C in the dark for 30 minutes. Similarly, the inhibitors of MRP1 (1mM probenecid and 100µM indomethacin) was added and the accumulation of calcein was measured. After the incubation period, the cells were pelleted by centrifugation at 5000rpm for five minutes. To the pellet, 500µl of PBS containing 0.1% BSA was added and analysed immediately by flow cytometry.

ATPase activity of MRP1

ATPase activity of MRP1 in Y79 RB cells was measured by the end point Pi release assay. 100µg/ml concentration of protein was incubated 2.5mM sodium fluoride and 0.2mM beryllium sulfate for 5 minutes at 37°C. Following incubation, different concentration of curcumin in the presence and absence of quercetin (10µM) was added and incubated for 3 minutes at

37°C. The reaction was initiated by the addition of 5mM ATP and terminated with 2.5% concentration of SDS after 20 minutes of incubation. The amount of Pi released was quantified using colorimetric method. MRP1-specific activity was recorded as the BeFx-sensitive ATPase activity.

Photoaffinity labelling of MRP1 with 8-azido-ATP-biotin

Crude membranes of MRP1 expressing Y79 RB cells (100µg protein) were incubated with 5mM MgCl₂ and 100µM 8-azido-ATP-biotin in the dark on ice for 5 min in the presence and absence of 10µM curcumin. The mixture was photolinked using UV light for 10 minutes. Immunoprecipitation of the photolinked sample was performed using MRP1 monoclonal antibody linked to protein A immobilized on agarose. Further, the immunoprecipitated protein was blotted and visualized with streptavidin horseradish peroxidase.

Statistical analysis

All experimental data were expressed as the mean ± Standard Deviation (SD) from triplicate samples of three independent experiments. Statistical analyses were performed by one-way analysis of variance (ANOVA) using SPSS 11.0 software. Values of p<0.05 were considered statistically significant.

In silico Analysis

Three dimensional structure of MRP1 have not been elucidated yet. Hence, homology search was performed for MRP1 amino acid sequence (UniProt ID: P33527) using BLASTp against Protein Data Bank (PDB) to identify the suitable templates towards modelling of MRP1 structure. Homology search results revealed that homodimeric multidrug exporter Sav1866 (PDB ID: 2HYD) of *Staphylococcus aureus* [11] as a suitable template, as it shared an overall sequence identity of 28% and similarity of 49% with MRP1. Further, for generating the homology model of MRP1, sequence alignment with Sav1866 was produced using ClustalW2 with default parameters. Further, based on this alignment, the three dimensional structure of MRP1 was generated using Modeller9v8 [12]. Among the 100 decoys generated for MRP1, the one with significant molecular Probability Density Function (PDF) and Discrete Optimized Potential Energy (DOPE) [13] was subjected to refinement. Further, the modelled structure was energy optimized through GROMACS 4.3.1, molecular dynamics package [14, 15]. The optimized model was evaluated for the stereo chemical aspects using PROCHECK [16] and for the energy profile using ProSA II server [17]. The structural quality of the protein was further evaluated by comparing the topology of the protein through structural superposition. The more sensitive TM-score was generated using TM align to check the probability of proteins sharing the same fold at the structural level. TM-Score > 0.17 is suggestive of a model and template sharing the similar topology [18].

The possible ligand binding cavities within the generated model was predicted using castP server [19]. The structural coordinates of curcumin (ACD0022) was retrieved from Indian Plant Anticancer Compound Database [20] and geometry optimized using PRODRG2 sever [21].

Molecular Docking simulation was carried out using AutoDock 4.2. Initially, the energy optimized protein and the ligand were prepared for docking by adding polar hydrogens. Further, the

protein and the ligand were also optimized by adding Kollman united atom charges and Gasteiger charges, respectively. Flexibility of the ligand was assigned based on its torsional degrees of freedom through Autotors, with the protein fixed to rigid throughout the process of docking simulation [22, 23]. Grid box covering the complete binding cavity as predicted using CASTp for MRP1 (104×104×104; 0.667Å) was built and the same was used for docking process. Further, Grid maps were generated for each atom within the ligand of MRP1 using Autogrid. Docking calculation was performed using Lamarckian genetic algorithm with default parameters, except for the number of GA runs which was set to 100. Further, cluster analysis was performed with a threshold RMSD set to 2.0Å to find the optimal binding orientation of the ligands. Potential binding pose of curcumin with MRP1 was predicted based on the binding energy and inhibitory constant. Finally, bonded and non-bonded interactions were also analyzed and visualized using PyMOL [24]. All the major structural bioinformatics tools used in this study were run on Open Discovery Linux platform [25] installed in Dell Precision workstation.

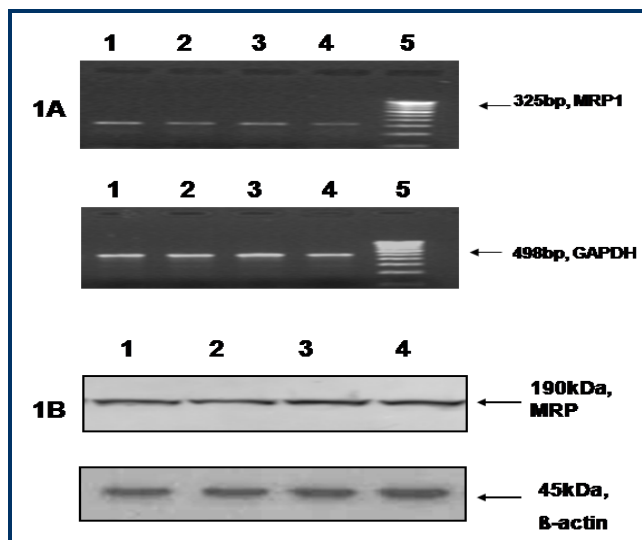


Figure 1: Effect of curcumin on MRP1 mRNA and protein expression in RB cell line: Dose-dependent effect of curcumin (2, 5, 10μM) after 72hrs on the MRP1 mRNA and protein expression in Y79 RB cells. (A) MRP1 and GAPDH expression in the Y79 RB cells. (B) MRP1 and beta actin expression in RB cells. Lane 1: Control cells, Lane 2: 2μM curcumin, Lane 3: 5μM curcumin, Lane 4: 10μM curcumin and Lane 5: Molecular weight marker. Both mRNA and protein level of MRP1 in curcumin treated was similar to the DMSO treated control, indicating that curcumin did not affect the expression level of MRP1.

Results:

Effect of curcumin on MRP1 expression in RB cell line

The Y79 RB cells treated with different concentrations of curcumin (2, 5 and 10μM) for 72 hours were detected by RT-PCR and western blot. It was found that the mRNA and protein level of MRP1 was similar to that of DMSO treated control RB cells, indicating absence of curcumin's effect on MRP1 expression (Figure 1A&B).

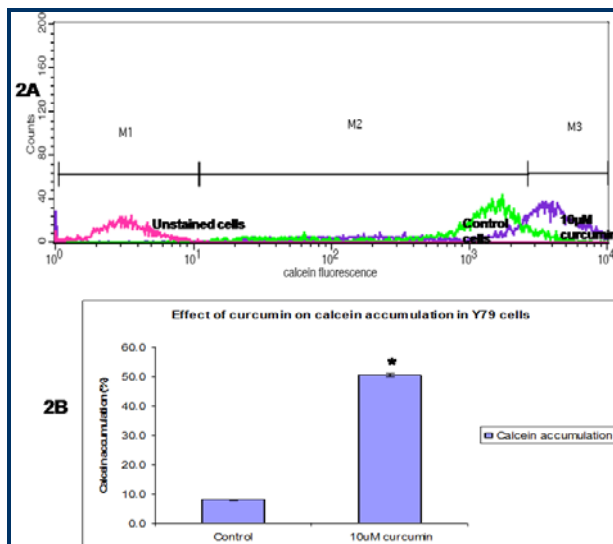


Figure 2: MRP1 functional activity in the Y79 RB cells: (2A) Effect of curcumin on MRP1 function was assessed by measuring the accumulation of fluorescent substrate calcein-AM. Histogram showing peak in pink color represents (unstained cells), green color (control cells) and blue color represents (10μM curcumin treated cells). (2B) Calcein accumulation is shown as bar diagram for n=3 experiments and are expressed as the mean ± S.D. * p<0.05, significantly different from the control.

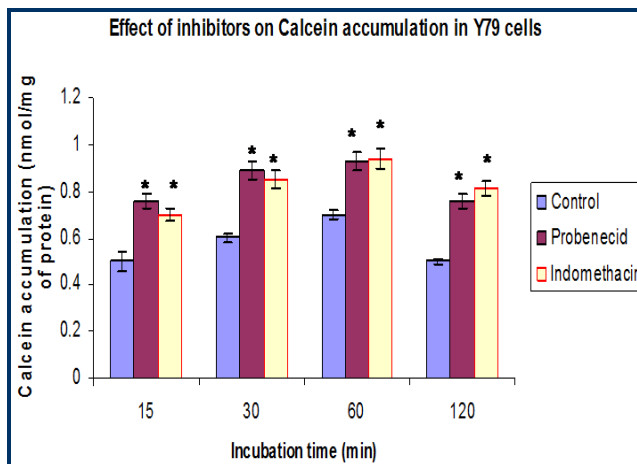


Figure 3: Effect of MRP1 inhibitors on calcein accumulation in Y79 RB cells: Y79 cells were incubated with and without inhibitors (100μM indomethacin and 1mM probenecid) and the calcein accumulation was observed at different time intervals. Data are expressed as the mean ±S.D for n=3 experiments.* p<0.05 significantly different from the control.

Effect of curcumin on MRP1 function by flow cytometry

The effect of curcumin on the MRP1 transport was tested by the accumulation of the fluorescent substrate calcein-AM using flow cytometry. The Y79 cells were incubated with calcein-AM and the intensity of fluorescence substrate accumulated was measured by FACS. Accumulation of fluorescent substrate was found to be increased (to nearly 50%) in the curcumin treated cells, when compared with the controls (Figure 2A and B). Similarly, indomethacin and probenecid (MRP1 inhibitors)

caused a significant increase in calcein accumulation at different time intervals in Y79 cell lines, which shows the involvement of MRP1 calcein efflux [Figure 3], and the results were also found to be statistically significant with $p < 0.05$.

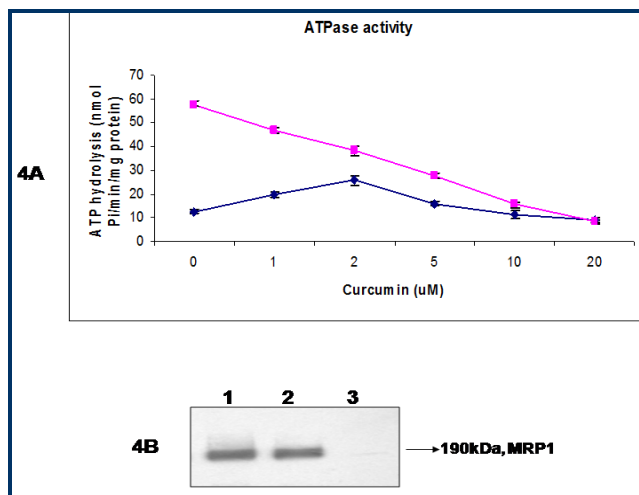


Figure 4: Effect of curcumin on basal and quercetin stimulated ATPase activity and photoaffinity labeling of MRP1 with 8-azido-ATP-biotin: (4A) Y79 cells expressing MRP1 (100µg of protein/ml) were incubated with increasing concentration of curcumin in the presence and absence of quercetin in the ATPase assay buffer. The reaction was initiated by the addition of 5mM ATP and terminated with 2.5% concentration of SDS after 20 minutes of incubation; the amount of Pi released was quantitated by colorimeter. (●) MRP1 basal activity; and (■) quercetin-stimulated MRP1 ATPase activity in the presence of different concentration of curcumin. Value represents \pm SE from at least three independent experiments. (4B) Crude membranes of (100µg protein) were incubated with 100µM 8-azido-ATP-biotin in the dark on ice for 5 min in the presence and absence of 10µM curcumin. The proteins were then immunoprecipitated with MRP1 antibody linked to agarose protein A beads. The immunoprecipitated protein was blotted and visualized with streptavidin horseradish peroxidase. The addition of 10mM ATP prevented photolabeling. Lane 1: 8-azido-ATP-biotin, Lane 2: 10µM curcumin and Lane 3: 10mM ATP.

Effect of curcumin on ATPase activity of MRP1

ATPase activity of MRP1 in the presence of curcumin was studied to assess the effect of curcumin on this transporter. Our results show that curcumin was able to stimulate the basal ATPase activity of MRP1 at very low concentration, but inhibited the activity at higher concentration. This is indicative of curcumin's direct interaction with the MRP1. Moreover, we also observed the inhibition of quercetin stimulated ATP hydrolysis by MRP1, mediated by curcumin in Y79 RB cell lines [Figure 4A].

Effect of curcumin on photoaffinity labelling of MRP1 by 8-azido-ATP-biotin

To determine the interaction sites of MRP1 with curcumin, photoaffinity labelling of MRP1 was performed using 8-azido-ATP-biotin. Curcumin had no effect on 8-azido-ATP-biotin of MRP1 at 10µM concentration in Y79 RB cell line. The cross linking of 8-azido-ATP was inhibited in the presence of 10mM ATP. This suggests that curcumin produce their effect most

likely by interacting at the substrate binding sites rather than at the nucleotide-binding sites of the MRP1 protein [Figure 4B].

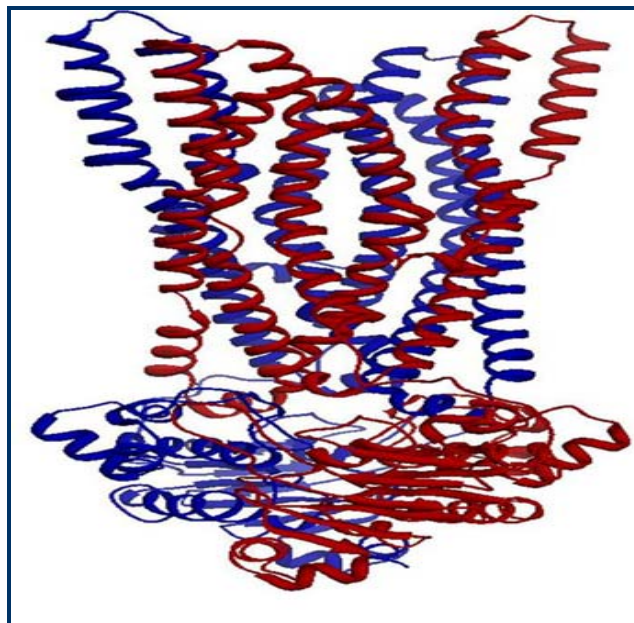


Figure 5: Homology based three dimensional model of MRP1.

Homology Modeling of MRP1

Among the experimentally determined structures of ABC transporter super family, SAV1866 (PDBID: 2HYD) of *Staphylococcus aureus* was found to be an appropriate template for human MRP1 with optimal query coverage (300-1531). Thus, three dimensional structure of human MRP1 was generated based on the molecular modeling protocol implemented by M. K. DeGorter *et al* [26]. The generated structural co-ordinates of human MRP1 was geometry optimized with a potential energy of $-1.6761530e+05$ kJ/mol. The resultant 3D structure of human MRP1 is predominantly helical in TM domains and β -sheets in the NBDs (Figure 5A). The overall stereo chemical aspects of MRP1 were inspected through Ramchandran plot, in which 91.0% of the residues in the most favoured region with no residues in disallowed region. Moreover, the overall quality of the model was further ascertained to be good with a Z-score of -6.02 as calculated using ProSA. TM-score of 0.93037 was calculated using the more sensitive structural alignment algorithm, TM-align. This score was suggestive of the generated model to share the same topology of the template with high probability. Hence, the model validated at the geometrical and energetic aspects ensure the plausibility for future analysis.

Binding cavity analysis

Binding site residues of MRP1 were predicted using CASTp (Table. 2 see supplementary material). The binding cavity of volume and area with 25694 and 9954.7, respectively were considered for the study. The amino acids residing in this cavity were documented to be involved in binding and transport of substrates [27].

Molecular Docking of MRP1 with curcumin and ATP

Molecular docking studies were performed for the optimized three dimensional structure of MRP1 with curcumin using LGA, to infer its binding mode. Among the conformers

generated, potential pose with lowest binding energy and highest binding affinity was selected for analysis. Curcumin showed bonded and non-bonded interactions with the substrate binding site of MRP1 with the binding energy and inhibitory constant of -7.39 kJ/mol and $3.82\mu\text{M}$, respectively. Further, interaction analysis of MRP1 with curcumin showed hydrogen bonding interactions Tyr384, Gln450 and Arg1249 and non bonded interactions with Tyr324, Phe385, Met443, Ser446, Ala447, Ile598, Val1194, Trp1198, Val1248 and Ser1252 (Figure 6A) (Table 3, see supplementary material).

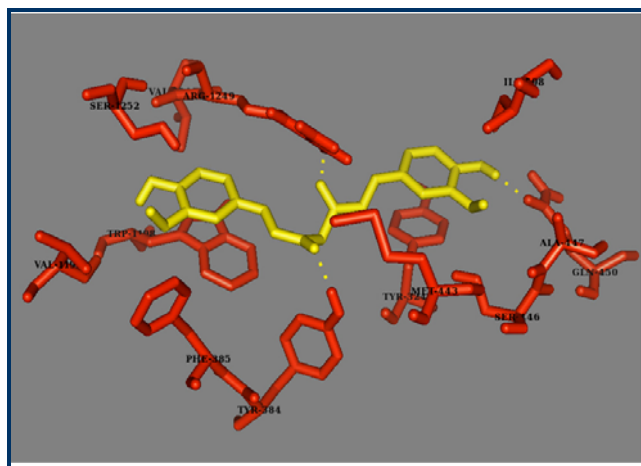


Figure 6: Molecular interaction observed between MRP1 with Curcumin. Binding site residues (RED) of MRP1 and Curcumin (Yellow) represented in sticks. The bonded and non-bonded interactions are visualized through PyMOL with H-bonded interaction represented through yellow color dashed lines.

Discussion:

Curcumin is a polyphenolic compound derived from turmeric. Its ability to affect gene transcription and induce apoptosis in various animal models with particular relevance to cancer chemoprevention and chemotherapy patients is well documented [10]. It has been studied that curcumin also serve as inhibitors of ABC transporters [28]. Recent studies have shown that curcumin significantly lowered the MDR1 gene expression in KB-V1 cervical carcinoma cell line. Similarly, it increased the accumulation of Rhodamine 123 and inhibited its efflux in cells which over-express P-glycoprotein [29]. In the present study, we investigated the effect of curcumin on MRP1 expression and function in Y79 RB cells.

In our earlier study, we have performed MTT assay to determine the relative cytotoxicity of curcumin in the Y79 RB cell line (data not shown; [30]). The concentrations that were less toxic to cells were chosen for further experiments. When $2-10\mu\text{M}$ curcumin was added to the Y79 for 72 hours, no effect was observed on MRP1 mRNA and protein expression. Similar results were observed by Wanida *et al*, where no change in the expression of MRP1 was observed after curcumin treatment in HEK-293 cells [31]. Cellular accumulation and the efflux studies were performed in Y79 RB cells employing calcein-AM as substrate for MRP1. This substrate is a non-fluorescent and lipophilic acetoxymethyl ester of calcein that rapidly diffuses through the plasma membrane into cells. In the cytosol, calcein-AM is metabolized by esterase to calcein which is

effluxed by the MRP1 protein. In a previous study, curcumin was also found to inhibit MRP1 transport by increasing the accumulation of fluorescent substrate calcein-AM and fluo4-AM using flow cytometry HEK-293 cells [31]. In the present study, we also found that there was a 30% increase in the accumulation of fluorescent substrate calcein-AM on curcumin treated Y79 cells by flow cytometry analysis. Similarly, indomethacin and probenecid (MRP1 inhibitors) caused a significant increase in calcein accumulation at different time intervals in Y79 cell lines, which show that MRP1 is involved in the efflux of calcein. Exposure to drug substrates can lead to stimulation or inhibition of ATPase activity of the ABC transporters [32]. Similar to P-gp [29], we found that curcumin was able to stimulate the ATPase activity of MRP1 at low concentration, but there was an inhibition of activity at higher concentration, which can be attributed to curcumin's interaction with MRP1's binding site. Further, our results also showed the inhibitory activity of curcumin on quercetin stimulated ATP hydrolysis by MRP1 in a dose dependent manner. Recently, Heleen *et al* also showed the inhibitory activity of curcumin on both MRP1 and MRP2 mediated transport in MDCKII cells, and it was also demonstrated that glutathione dependent metabolism of curcumin to play an important role in MRP1 inhibition [9]. To ascertain the probable curcumin interaction sites on MRP1, photoaffinity labeling of MRP1 was performed. This was done using 8-azido-ATP-biotin, an analog of ATP, which has been already to bind specifically to the nucleotide binding domain of P-gp and MRP [31]. Subsequently, in the post labelling experiments we found the lack of curcumin's effect on 8-azido-ATP-biotin binding to MRP1 at $10\mu\text{M}$ concentration in Y79 cell lines. This suggests that curcumin produces its effect most likely by interacting at the substrate binding sites rather than at the nucleotide-binding sites of the MRP1 protein to modulate ATP hydrolysis.

It has been documented through mutational studies that the residues spanning (Transmembrane) TM11 (Ile598) and TM17 (Val1248) are the regions involved in substrate binding and its transport. Further, retention in the transport activity was observed on mutating Phe385, Trp1198 and Arg1249, which signifies the biological importance of these residues on substrate transport [25]. In the present study, docking interaction analysis of MRP1-curcumin complex showed network of bonded and non bonded interactions with Curcumin to the amino acid residues residing in the documented substrate binding region. Docking studies also inferred that oxygen atoms of phenolic and methoxy functional groups spanning terminal phenyl rings of curcumin to play a crucial role for inhibitory action.

Conclusion:

Multi-drug resistance in tumour cells is a significant impediment to the success of chemotherapy in many cancers. Curcumin, a natural polyphenolic compound has led to scientific interest in its ability as a chemotherapeutic agent. Our *in vitro* results showed the potential of curcumin in modulating the function and expression of multi-drug resistance proteins MRP1. Furthermore, *in silico* molecular docking studies of these MDR proteins with curcumin provides an insight on the active binding mode of curcumin. Thus, curcumin can be used as a promising MDR chemosensitizer in modulating the multidrug resistance property in various cancers.

Conflict of interest

The authors declare that they have no conflict of interest.

Acknowledgement

The present work was supported by grant from Indian Council of Medical Research (5/13/25/04/NCD-III).

References:

- [1] Ishikawa Y & Nagai J *Biol Pharm Bull.* 2010 **33**: 504 [PMID: 20190417].
- [2] Krishnakumar S *et al. Br J Ophthalmol.* 2004 **88**: 1521 [PMID: 15548804].
- [3] Squire J *et al. Hum Genet.* 1985 **70**: 291 [PMID: 4018796].
- [4] Van Brussel JP *et al. Eur J Cancer.* 1999 **35**: 664 [PMID: 10492644].
- [5] Liu YH *et al. Clin Exp Pharmacol Physiol.* 2010 **37**: 115 [PMID: 19566819].
- [6] Chan HS *et al. Cancer Res.* 1997 **57**: 2325 [PMID: 9192801].
- [7] Dallas S *et al. Pharmacol Rev.* 2006 **58**: 140 [PMID: 16714484].
- [8] Levy C *et al. Br J Ophthalmol.* 1998 **82**: 1154 [PMID: 9924303].
- [9] Wortelboer HM *et al. Chem Res Toxicol.* 2003 **16**: 1642 [PMID: 14680379].
- [10] Lin YG *et al. Clin Cancer Res.* 2007 **13**: 3423 [PMID: 17545551].
- [11] Dawson RJ *et al. Nature.* 2006 **443**: 180 [PMID: 16943773].
- [12] Eswar N *et al. Methods Mol Biol.* 2008 **426**: 145 [PMID: 18542861].
- [13] Shen MY & Sali A. *Protein Sci.* 2006 **15**: 2507 [PMID: 17075131].
- [14] Van Der Spoel D *et al. J Comput Chem.* 2005 **16**:1701 [PMID: 16211538].
- [15] Summa CM & Levitt M. *Proc Natl Acad Sci U S A.* 2007 **104**: 3177 [PMID: 17360625].
- [16] Laskowski RA *et al. J Appl Crystallogr.* 1993 **26**: 283 [doi:10.1107/S0021889892009944]
- [17] Wiederstein M *et al. Nucleic Acids Res.* 2007 **35**: W407 [PMID:17517781].
- [18] Xu J & Zhang Y. *Bioinformatics.* 2010 **26**: 889 [PMID: 20164152].
- [19] Liang J *et al. Protein Sci.* 1998 **7**: 1884 [PMID: 9761470].
- [20] Vetrivel *et al. Bioinformation* 2009 **4**: 71[PMID: 20198172]
- [21] Schüttelkopf AW *et al. Acta Crystallogr D Biol Crystallogr.*2004 **60**: 1355[PMID: 15272157].
- [22] Goodsell DS *et al. J Mol Recognit.* 1996 **9**: 1[PMID: 8723313].
- [23] <http://www.pymol.org/>.
- [24] Vetrivel U & Pilla K, *Bioinformation.* 2008 **3**: 144 [PMID: 19238235].
- [25] Corbeil CR *et al. J Chem Inf Model.* 2007 **47**: 435 [PMID: 17305329].
- [26] DeGorter MK *et al. Biochem Biophys Res Commun.* 2008 **365**: 29 [PMID: 17980150].
- [27] Deeley RG *et al. Physiol Rev.* 2006 **86**: 849 [PMID: 16816140].
- [28] Chearwae W *et al. Mol Cancer Ther.* 2006 **5**: 1995 [PMID: 16928820]
- [29] Zhou S *et al. Drug Metab Rev.* 2004 **36**: 57 [PMID: 15072439]
- [30] Thiyagarajan S *et al. Curr Eye Res.* 2009 **34**: 845 [PMID: 19895312]
- [31] Chearwae W *et al. Cancer Chemother Pharmacol.* 2006 **57**: 376 [PMID: 16021489].
- [32] Sauna ZE *et al. J Biol Chem.* 2004 **279**: 48855 [PMID: 15364914]

Edited by P Kanguane

Citation: Sreenivasan *et al. Bioinformation* 8(1): 013-019 (2012)

License statement: This is an open-access article, which permits unrestricted use, distribution, and reproduction in any medium, for non-commercial purposes, provided the original author and source are credited.

Supplementary material:

Table 1: Table shows the PCR primers used in the gene expression studies

Gene	Primer sequences (3'-5')	Annealing temp. °C	PCR product size
MRP1	FP CGTCTACTCCAACGCTGAC	57°C	325bp
	RP CTGGACCGCTGACGCCCGTGAC		
	FP GCCAAGGTCATCCATGACAAC		
GAPDH	RP GTCCACCACCCTGTTGCTGTA	63°C	498bp

Table 2: Binding Cavity predicted through Computed Atlas of Surface Topography of proteins (CASTp)

Protein	Area (Å ²)	Volume (Å ³)	Residues spanning in the predicted binding cavity
MRP1	9954.7	25694	W309,K319,G322,P323,Y324,F325,M327,S328,F329,F330,F331,K332,A333,I334,H335,D336,L337,M338,M339,L369,V372,T373,Q377,V380,L381,Y384,F385,C388,F389,V390,S391,G392,M393,K396,V424,N425,S428,V429,Q432,R433,F434,M435,D436,L437,A438,T439,Y440,N442,M443,I444,W445,S446,A447,P448,Q450,L453,A454,V479,N480,M483,T487,Q491,H494,M495,K498,R501,I502,R532,E535,L536,K537,L539,S542,A543,L545,S546,A547,V548,G549,T550,F551,T552,W553,V554,C555,P557,F558,L559,V560,A561,L562,A587,L588,F589,N590,I591,L592,R593,F594,P595,L596,N597,I598,L599,P600,M601,V602,I603,S604,S605,I606,Q608,A609,V611,S612,F982,N985,H986,V987,S988,A989,L990,A991,S992,N993,Y994,W995,L996,S997,W999,G1032,Y1033,S1034,M1035,A1036,V1037,S1038,I1039,G1040,G1041,I1042,L1043,S1045,R1046,C1047,L1048,H1049,V1050,D1051,L1053,H1054,L1057,L1080,V1083,D1084,S1085,M1086,I1087,P1088,E1089,V1090,I1091,K1092,F1094,M1095,G1096,F1099,N1100,V1101,I1102,G1103,A1104,V1107,L1110,S1137,R1138,Q1139,L1140,K1141,E1144,S1145,R1148,Y1152,K1187,Y1190,P1191,I1193,V1194,A1195,R1197,W1198,V1201,R1202,L1203,E1204,C1205,V1206,G1207,N1208,L1212,V1234,S1235,S1237,L1238,Q1239,T1241,T1242,Y1243,L1244,N1245,W1246,L1247,V1248,R1249,M1250,S1251,S1252,E1253,M1254,E1255 and T1256

Table 3: Significant Molecular interactions observed between MRP1 and Curcumin. Residues involved in H-bond interactions were bolded.

Protein	Predicted Binding Energy (kJ/mol)	Inhibitory constant (Ki)	Interacting Residues (Bonded and Non bonded contacts)
MRP1-Curcumin	-7.39	3.82µM	Tyr324, Tyr384 ,Phe385,Met443,Ser446, Gln450 ,Ala447,Ile598,Val1194,Trp1198,Val1248, Arg1249 and Ser1252